Concentration Fluctuations in Entangled Polymer Solutions near the Liquid−Liquid Phase Separation Temperature

Taco Nicolai*

Chimie et Physique des Matériaux Polymères, UMR CNRS, Université du Maine, 72085, Le Mans Cedex 9, France

Wyn Brown

Department of Physical Chemistry, University of Uppsala, Box 532, 751 21 Uppsala, Sweden

Received November 25, 1998; Revised Manuscript Received January 26, 1999

ABSTRACT: Solutions of polyisobutylene (PIB) in ethyl caprylate were investigated using mechanical shear measurements and dynamic and static light scattering. By varying the polymer concentration, the effect of entanglements on the amplitude and the dynamics of concentration fluctuations was studied over a range of temperatures from the phase separation temperature (T_{ps}) up to 30 deg above the θ temperature. While the time-averaged scattered intensity is not influenced by entanglements, dynamic light scattering shows that the relaxation of the concentration fluctuations close to T_{ps} is dominated by the viscoelastic relaxation of the transient polymer network. The results are interpreted in terms of existing theory on the influence of the elastic modulus on the relaxation of concentration fluctuations.

Introduction

Critical density fluctuations in pure liquids and liquid mixtures have been studied extensively using light scattering.[1] The experimental results are in good agreement with theory. Critical concentration fluctuations in polymer solutions are less investigated.[2] Nevertheless, it is clear that polymer solutions belong to the same universality class as blends of small molecules.[2] However, in most studies the polymers were not entangled. This paper reports the first light scattering study of the effect of entanglements on critical fluctations.

Entanglements are the origin of the high viscosity of semidilute solutions of large polymers.[3] It has been shown both experimentally[4] and theoretically[5] that entanglements can have a strong influence on the dynamics of concentration fluctuations as probed by dynamic light scattering (DLS). The relaxation of spontaneous concentration fluctuations measured by DLS is driven by the longitudinal modulus (M). M contains contributions from the osmotic (M_{os}) and the elastic (M_{el}) modulus. The relative amplitudes of the two moduli depend on the solvent quality and thus on the temperature close to and below the θ temperature. In good solvents $M_{os} \gg M_{el}$ so that the effect of entanglements on the relaxation of concentration fluctuations is small. On the other hand, close to the temperature where phase separation occurs (T_{ps}) $M_{el} \gg M_{os}$ so that the effect of entanglements is very strong. The importance of the effect of entanglements on critical fluctuations was noted by Tanaka,[6] who gave a theoretical treatment.

If the strengths of the two moduli are of the same order of magnitude, the relaxation of both the osmotic and elastic moduli can be observed in a DLS experiment. A relatively fast, narrow, q^2-dependent, mode characterizes the relaxation of the osmotic modulus, while a relatively slow broad, q-independent, mode characterizes the relaxation of the elastic modulus. It was shown[7] that the relative amplitude of the slow mode increases with decreasing solvent quality. The concentration and molar mass dependence of the second mode were found to be the same as that of the terminal relaxation time of the shear modulus.[7]

In this paper we investigate the effect of entanglements on both the amplitude and the dynamics of concentration fluctuations when approaching the phase separation temperature. We do not attempt to determine the critical scaling exponents with high accuracy or the crossover from mean field to critical behavior. Such measurements are very demanding and difficult even for well-defined model systems. We focus here on the effect of entanglements by comparing solutions with different polymer concentrations and thus different entanglement densities. To clearly see the effect of entanglements in polymer solutions close to the critical concentration, we need to use very flexible polymers with high molar mass. In this study we used polyisobutylene (PIB) in ethyl caprylate. The advantages of using this rather unconventional solvent are that it has a convenient θ temperature ($T_\theta = 22$ °C[8]), and it is not volatile which facilitates mechanical measurements.

Experimental Section

Apparatus. Mechanical shear measurements were done on a stress-controlled rheometer (Contraves low shear 40) using the Couette geometry. The temperature was set with a thermostat bath to within ±0.2 °C. The applied stress was small enough to ensure that the measurements were done in the linear response regime. Static and dynamic light scattering measurements were done using an ALV-5000 multibit, multi-τ full digital correlator in combination with an Ar ion laser emitting vertically polarized light with wavelength 488 nm. The temperature was set with a thermostat bath to within ±0.1 °C.

Sample Preparation and Characterization. The PIB fraction was a gift from BASF (Ludwigshafen). PIB was first dissolved in heptane in dilute solution (<0.05%) and filtered through Millipore filters (0.45 μm) to remove dust. Then the volume of heptane was reduced by evaporating off at 30 °C, the vessel being sealed with a filter. Then the desired amount of ethyl caprylate (Aldrich, 99+% pure) was added to make a given solution, and the rest of the heptane was evaporated off to constant weight. Ethyl caprylate has a very low vapor

10.1021/ma9818329 CCC: $18.00
Published on Web 03/25/1999

pressure and did not evaporate significantly. This method assured that the polymer was kept in solution at all times.

A dilute PIB solution (0.118 g/L) was characterized in ethyl caprylate using static and dynamic light scattering. The relative excess scattered intensity (I_r) is defined as the scattering intensity of the solution minus the solvent scattering divided by the scattering intensity of toluene at 25 °C. At very low concentrations interactions can be neglected so that the weight-average molar mass (M_w) and the *z*-average radius (R_{gz}) can be calculated using the Zimm approximation valid for $qR_g < 1$:[9]

$$\frac{Kc}{I_r} = \frac{1}{M_w}\left[1 + \frac{(qR_{gz})^2}{3}\right] \quad (1)$$

where $q = [4\pi n \sin(\theta/2)]/\lambda$ is the scattering wave vector, θ is the angle of observation, n is the refractive index, and $K = (4\pi^2 n_{tol}^2/\lambda^4 N_a R_{tol})(dn/dc)^2$. N_a is Avogadro's number. We have used $R_{tol} = 3.1 \times 10^{-5}$ cm^{-1} for the Rayleigh ratio of toluene at 25 °C.[11] We determined the refractive index increment of PIB in ethyl caprylate at 298 K and found $dn/dc = 0.107$ cm^3/g. In the following we neglect the temperature variation of the parameters used in the calculation. At 293 K we obtained $R_{gz} = 165$ nm and $M_w = 9.1 \times 10^6$ g/mol by applying eq 1 to data at very low scattering angles (13°−θ−30°).

An apparent diffusion coefficient was calculated from the *z*-average relaxation rate (Γ_z) obtained from DLS:[10] $D_a = \Gamma_z/q^2$. At large q values D_a increases linearly with q due to contributions from relaxation of internal modes. At the smallest q values D_a becomes independent of q and corresponds to the translation diffusion coefficient (D_0). The *z*-average hydrodynamic radius (R_{hz}) can be calculated using the Stokes−Einstein relation: $D_0 = kT/(6\pi\eta R_{hz})$, with k Boltzmann's constant and η the solvent viscosity. We measured the viscosity of ethyl caprylate in the range 283 K < T < 353 K: $\log(\eta) = [207/(T + 143)] - 1.086$. At 293 K we obtained $R_{hz} = 85$ nm. The high ratio R_{gz}/R_{hz} is to a large extent due to the size polydispersity of the sample. Since $R_{gz} = \langle R_g^2\rangle_z^{1/2}$ and $R_{hz} = 1/\langle R_h^{-1}\rangle_z$, large sizes are more strongly weighted in R_{gz} than in R_{hz}.

The size distribution of the PIB sample was determined in THF using size exclusion chromatography. The columns used (Polymer Laboratories E-lin 10 μm and MIX-B 10 μm, each 600 × 7.5 mm, in series) are adapted for separation of large polymers. No filter and precolumn were used to minimize shear degradation. The results show that the sample has a pronounced low molar mass tail leading to a large polydispersity index ($M_w/M_n \approx 5$).

The overlap concentration defined as $C^* = 3M_w/(4\pi N_a R_{gz}^3)$ is equal to 0.9 g/L. However, for polydisperse samples such a calculation of the overlap concentration is only a rough estimation. With number-average values for the molar mass and the radius of gyration the calculated value of C^* is larger by at least a factor 3.

Results and Discussion

Shear Modulus. We measured the frequency dependence of the loss (G'') and storage (G') shear moduli of four solutions with concentrations 5.0, 7.8, 15, and 18.8 g/L at temperatures between T_{ps} and 333 K. Figure 1 shows master curves of G' and G'' as a function of the radial frequency. These master curves were obtained using time−temperature superposition. No vertical shifts were necessary because the temperature dependence of the plateau modulus ($G_0 \propto T/T_{ref}$) is small in the temperature range used. Horizontal shifts were slightly larger than expected from the temperature dependence of the solvent viscosity. Very close to T_{ps} the viscosity of the samples drops dramatically. When the temperature is again increased, the original viscosity is recovered after several hours.

It is clear from Figure 1 that the viscoelastic relaxation is very strongly concentration dependent in this concentration range. However, it is possible to superimpose the data obtained at different concentrations using horizontal and vertical shift factors; see Figure 2. This means that the shape of the terminal relaxation process due to disentanglement is within experimental error the same at least for the three higher concentrations. For the lowest concentration we observe mainly liquidlike behavior in the frequency−temperature range covered. For this concentration the shift factors are uncertain due to the large scatter in G''. The solid lines in Figure 2 indicate the slopes of G' and G'' for purely viscous response: $G' \propto \omega^{-2}$ and $G'' \propto \omega^{-1}$. The shapes of the $G'(\omega)$ and $G''(\omega)$ are characteristic for entangled polymers although the transition from liquidlike behavior at low frequencies to rubberlike behavior at high frequencies is very broad due to the polydispersity of the sample. In fact, even for the highest concentration we can hardly detect a plateau modulus for G' and a maximum for G'' in the frequency−temperature range covered. In view of the broad relaxation time distribution of the disentanglement process any choice of a characteristic relaxation time (τ_{el}) is arbitrary. If one takes τ_{el} as the inverse radial frequency where the solid

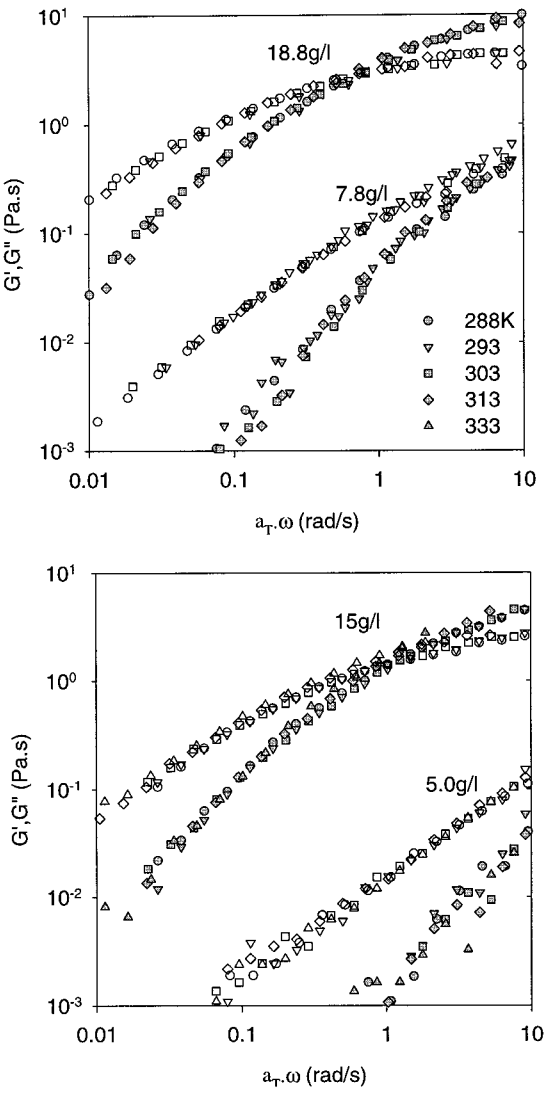

Figure 1. Frequency dependence of the loss (open symbols) and storage (closed symbols) shear moduli at different concentrations. The master curves were obtained by superposition of measurements at different temperatures indicated in the figure. The reference temperature is 293 K.

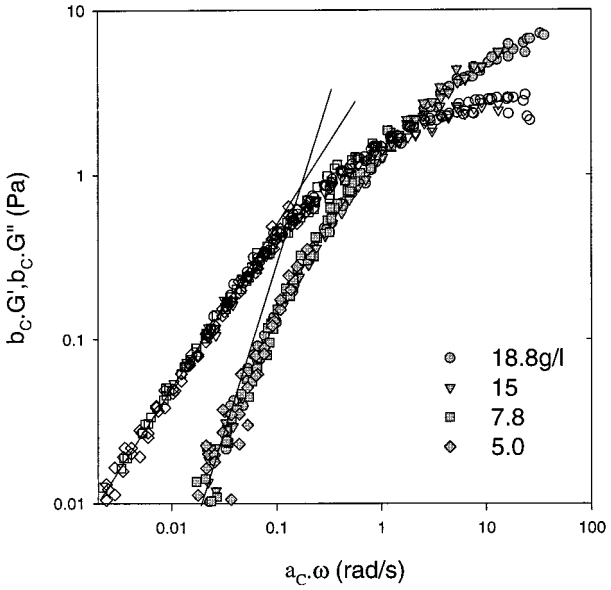

Figure 2. Superposition of the data shown in Figure 1 using both horizontal and vertical shift factors. $a_C = 0.67$, 1, 3.2, 3.2 and $b_C = 2.5$, 1, 0.11, 0.010 for $C = 18.8$, 15, 7.8, and 5.0 g/L, respectively. The solid lines give the limiting low-frequency dependence: $G' \propto \omega^2$ and $G'' \propto \omega$.

lines in Figure 2 cross, we obtain at 293 K $\tau_{el} = 17$, 7, 0.7, and 0.07 s for $C = 18.8$, 15, 7.8, and 5.0 g/L, respectively. We can roughly estimate the values of the plateau modulus of the mastercurve and use the shift factors to calculate the values at lower concentrations: $G_0 = 15$, 10, and 3 Pa for $C = 18.8$, 15, and 7.8 g/L. The viscosities obtained from $\eta = G''/\omega$ at low frequencies are 16.8, 4.5, 0.16, and 0.014 Pa·s for $C = 18.8$, 15, 7.8, and 5.0 g/L, respectively.

Static Light Scattering. We investigated four solutions with concentrations 15, 7.8, 5.0, and 2.8 g/L at temperatures between T_{ps} and 333 K. For more concentrated solutions the relaxation of the concentration fluctuations is too slow to obtain good time averages within a few hours. The q dependence of the relative excess scattering intensity (I_r) could for all concentrations and temperatures be described by the so-called Ornstein−Zernike (OZ) equation:

$$I_r = I_r(0)[1 + (q\xi)^2]^{-1} \qquad (2)$$

Here $I_r(0)$ is the zero angle scattered intensity and ξ is the static correlation length of the concentration fluctuations. Equation 2 implies that if $1/I_r$ is plotted versus q^2, we obtain straight lines as is illustrated in Figure 3. However, straight lines are obtained in this representation for any structure factor ($S(q) = I_r/I_r(0)$) if $q\xi$ is small. Alternatively, one can plot $S(q)$ as a function of $q\xi$, which gives a universal curve for all temperatures and concentrations; see Figure 4. From such a representation it is clear that the OZ equation gives a good description of the data over the whole accessible $q\xi$ range. Very close to T_{ps} a small deviation from the OZ equation is expected,[1,2] but our data are not sufficiently precise to detect this deviation. At $T > T_\theta$ again a deviation from the OZ equation is expected due to excluded-volume interactions on length scales smaller that ξ. However, at high temperatures ξ is small so that we do not have access to large values of $q\xi$ where this deviation becomes significant.

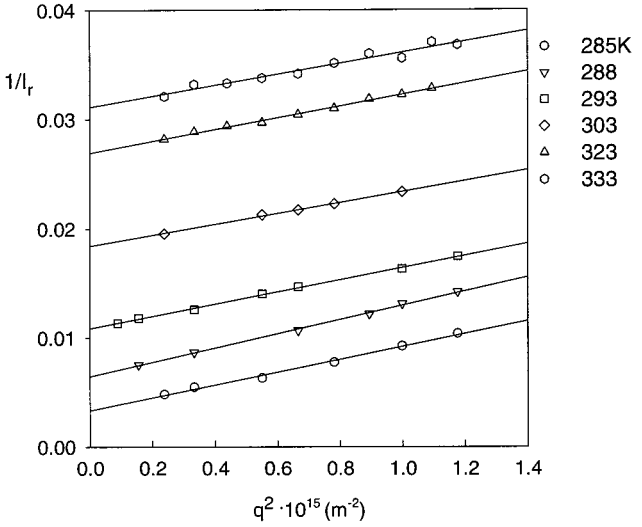

Figure 3. $1/I_r$ versus q^2 for 15 g/L PIB in ethyl caprylate at different temperatures indicated in the figure. The solid lines represent linear least-squares fits.

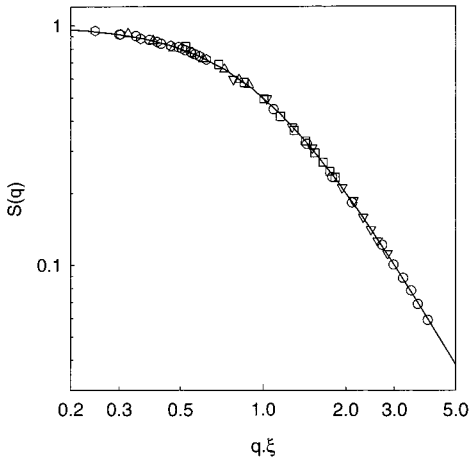

Figure 4. Double-logarithmic representation of the static structure factor ($S(q) = I_r/I_r(0)$) as a function of $q\xi$ for 7.8 g/L PIB in ethyl caprylate at different temperatures. The solid line represents the Ornstein−Zernike equation (eq 2). Symbols as in Figure 3.

The system can be considered as an ensemble of noninteracting particles (blobs) with apparent radius of gyration $R_a = \sqrt{3}\xi$ and apparent molar mass $M_a = I_r(0)/KC$. If the structure factor of the system is the same at different concentrations and temperatures, then $M_a = aR_a^{df}$ independent of T and C, with df the fractal dimension. The prefactor a depends on the structure of the polymer chains on the length scale below the persistence length. Figure 5 shows that scaling behavior is indeed observed within the experimental error. Again the data are not sufficiently precise to detect the small deviation from df = 2 expected very close to T_{ps}.[1,2] The effect of excluded-volume interactions at $T > T_\theta$ which leads to a slightly smaller fractal dimension is not significant in the temperature range investigated. The value 2 for df explains why the lines in Figure 3 are parallel ($\xi^2/I_r(0)$ is constant).

$I_r(0)/T$ is proportional to the susceptibility (χ) and is the sum of the contribution of critical fluctuations and noncritical concentration fluctuations (background). Theory predicts that the critical part diverges at T_{ps} as $(T - T_{ps})^{-\gamma}$ with $\gamma = 1.24$ in the nonclassical treatment valid very close to T_{ps} and $\gamma = 1$ in the classical

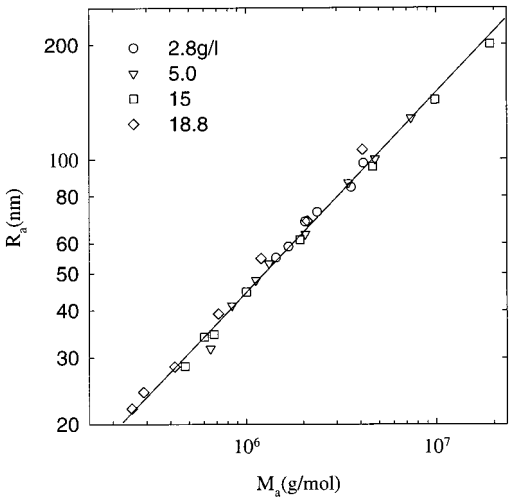

Figure 5. Double-logarithmic representation of the apparent molar mass versus the apparent radius of gyration for all concentrations and temperatures. The solid line has slope two.

treatment valid at higher temperatures.[1,2] The background term varies only weakly with temperature and dominates at $T \gg T_{ps}$. Figure 6 shows the temperature dependence of $I_r(0)/T$ and ξ for the solution with $C =$ 7.8 g/L. The solid and dashed lines represent nonlinear least-squares fits fixing γ to 1 and 1.24, respectively, while keeping the background, T_{ps}, and the prefactor as free fit parameters. It is clear that the data are not sufficiently precise to distinguish between the classical and nonclassical treatments. In fact, our lowest temperature data are probably in the crossover regime.[12] The divergence of ξ is directly related to that of $I_r(0)/T$ because $I_r(0) \propto \xi^2$.

Figure 7 shows that the divergence of $I_r(0)/T$ and thus ξ at T_{ps} is independent of the concentration in the range investigated. T_{ps} is 280, 284.5, and 281.5 K for C equal to 5, 7.8, and 15 g/L, respectively. The background term varies little for the concentrations used here. The critical concentration and temperature are thus about 8 g/L and 285 K, respectively. For the sample with $C = 2.8$ g/L we did not observe a divergence of $I_r(0)$ and ξ. Instead, we observed a modest increase of $I_r(0)$ and ξ down to $T =$ 283 K at which temperature the scattered light intensity increased very slowly in time. Probably phase separation occurs at this concentration via nucleation and growth as reported recently by Szydlowski and Van Hook.[13]

Dynamic Light Scattering. We measured the time-averaged intensity autocorrelation function ($\langle I(0)\, I(t)\rangle$) of the solutions as a function of q and T. The normalized intensity autocorrelation function ($g_2(t)$) is related to the electric field autocorrelation function ($g_1(t)$): $g_2(t) = 1 + \beta|g_1(t)|^2$, [11] where β takes into account deviations from ideal correlation. Since the scattering from density fluctuations is negligible, $g_1(t)$ is directly related to the relaxation of spontaneous concentration fluctuations.

The effect of viscoelastic relaxation on the dynamic structure factor has been investigated theoretically by several authors.[5] Qualitatively these theories state that spontaneous concentration fluctuations relax initially by a relative motion of the solvent with respect to the polymer driven by the osmotic modulus. This leads to a local swelling or deswelling of the transient network of entangled polymers. This first relaxation process stops when the osmotic modulus is exactly opposed by the elastic modulus. Further relaxation of concentration fluctuations can only occur by relaxation of the elastic modulus, i.e., disentanglement of the polymer chains.

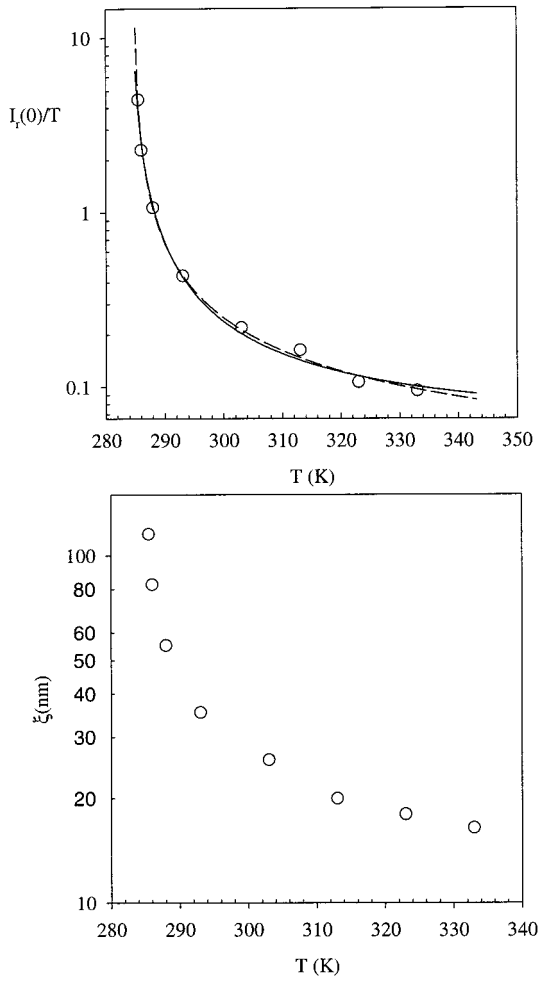

Figure 6. Semilogarithmic representation of the temperature dependence of $I_r(0)/T$ (top) and ξ (bottom) for 7.8 g/L PIB in ethyl caprylate. The lines represents a nonlinear least-squares fit to $I_r(0)/T = A(T - T_{ps})^{\gamma} + B$ with A, T_{ps}, and B free fit parameters and γ fixed to either the classical value ($\gamma = 1$, dashed line) or the critical value ($\gamma = 1.24$, solid line).

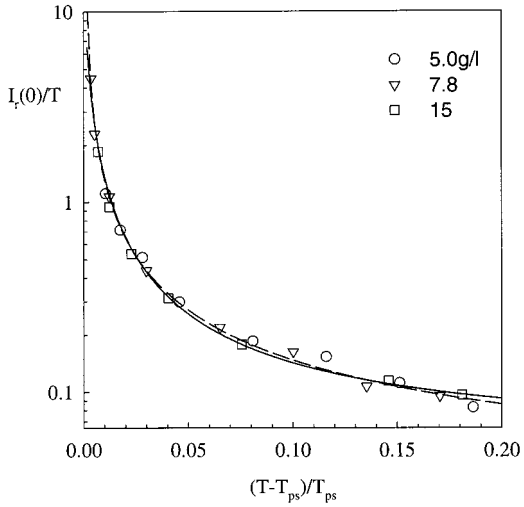

Figure 7. Semilogarithmic representation of the reduced temperature dependence of $I_r(0)/T$ for PIB in ethyl caprylate at three concentrations indicated in the figure. The dashed and solid lines are the same as in Figure 6.

The general expression of the dynamic structure factor which includes the time-dependent longitudinal elastic modulus is intricate. It is not straightforward to analyze experimental data in terms of this expression unless one has an analytical expression for the time dependence of the elastic modulus. The expression is much simplified if it is assumed that the elastic modulus is characterized by a single relaxation time (τ_{el}) much longer than the relaxation of the osmotic modulus. In this case $g_1(t)$ is simply the sum of two exponentials:

$$g_1(t) = A_1 \exp(-t/\tau_1) + A_2 \exp(-t/\tau_2) \qquad (3)$$

The relaxation rate of the fast mode is given by $\tau_1 = f/(Mq^2)$, where f is the friction coefficient, while that of the slow mode is given by $\tau_2 = \tau_{el}(M/M_{os})$. The ratio of the amplitudes equals the ratio of the moduli: $A_1/A_2 = M_{os}/M_{el}$. In reality, the elastic modulus is characterized by a broad distribution of relaxation times as is obvious from Figure 2. Earlier studies[7] of monodisperse polystyrene solutions in Θ solvents show a good quantitative correspondence between the terminal relaxation time of the shear modulus and that of the concentration fluctuations probed by DLS.

Figure 8 shows normalized correlation functions of the solutions at $T = 288$ K and $q = 1.25 \times 10^{-2}$ nm^{-1} ($\theta = 40$ deg). For the two higher concentrations the correlation function clearly contains two relaxation processes. The fast relaxation is attributed to the relaxation of the osmotic modulus while the slow relaxation corresponds to the relaxation of the elastic modulus. The relaxation time of the slow mode increases rapidly with increasing concentration in qualitative agreement with the increase of the relaxation time of the shear modulus. At the low concentrations the two modes merge.

Figure 9 shows the q dependence of the correlation functions for the sample with $C = 15$ g/L at $T = 288$ K. The relative amplitude of the slow mode does not vary significantly with q, but its relaxation time has a clear q dependence. This is not expected if the viscoelastic relaxation is much slower than that of the osmotic modulus. Earlier measurements of monodisperse polystyrene solutions in Θ solvents showed no q dependence of the slow mode. We tentatively attribute the q dependence observed for the present system to the large polydispersity. In addition, in the earlier measurements both $q\xi$ and qR_{gz} were smaller than unity in the whole q range covered which is not the case here.

The temperature dependence of the autocorrelation function is shown in Figure 10 for the solution with $C = 15$ g/L at $q = 1.25 \times 10^{-2}$ nm^{-1}. We corrected the time axis for variations of the solvent viscosity and the kinetic energy. The relative amplitude of the slow mode increases strongly as T approaches T_{ps}. This is expected as the relative amplitude of the slow mode is directly related to the relative strength of the elastic modulus. The temperature variation of the elastic modulus is weak while the osmotic modulus decreases strongly as we approach T_{ps}. The terminal relaxation time of the slow mode after correction for the solvent viscosity increases with decreasing temperature. Even though τ_{el} itself is not very sensitive to the temperature, the terminal relaxation time increases because M/M_{os} increases.

We have fitted the correlation functions both using an numerical inverse Laplace transformation and by imposing a bimodal distribution as discussed in ref 7. Although a good description of the data was obtained

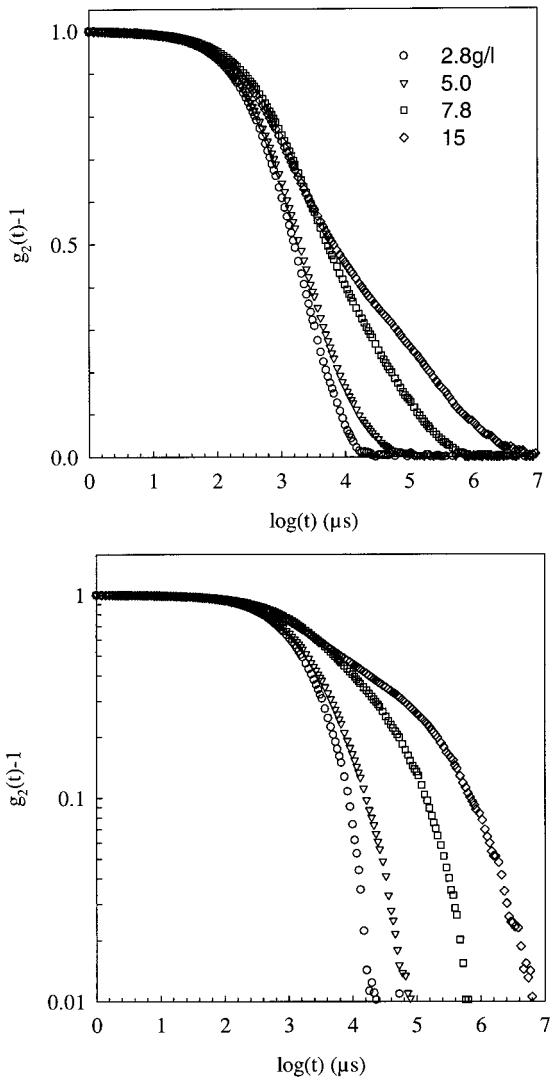

Figure 8. Semilogarithmic (top) and double-logarithmic (bottom) representations of the normalized intensity correlation functions of PIB in ethyl caprylate at different concentrations indicated in the figure with $T = 288$ K and $q = 1.25 \times 10^{-2}$ nm^{-1}.

by either procedure, we did not obtain unambiguous results for the relaxation times. The reason is that the slow mode is very broad and overlaps at short times with the fast mode. In view of this ambiguity in conjunction with the large polydispersity of the PIB sample, we only give a semiquantitative discussion of the DLS results.

There has been some discussion in the past whether the longitudinal modulus of the solution or of the transient polymer network should be used.[14] The latter is orders of magnitude smaller than the solution longitudinal modulus. In the first case coupling between density and concentration fluctuations is assumed essential.[15] We believe that only the elastic modulus of the transient network is important and that the density fluctuations are not coupled to the concentration fluctuations in the systems investigated here. The elastic longitudinal modulus of gels is about the same as the shear modulus.[16] The osmotic modulus is related to the osmotic compressibility ($M_{os} = C(d\pi/dC)$) and can be calculated from the time-averaged light scattering intensity: $I_r(0) = KRTC^2/M_{os}$, where K is a constant depending on the scattering contrast (see Experimental

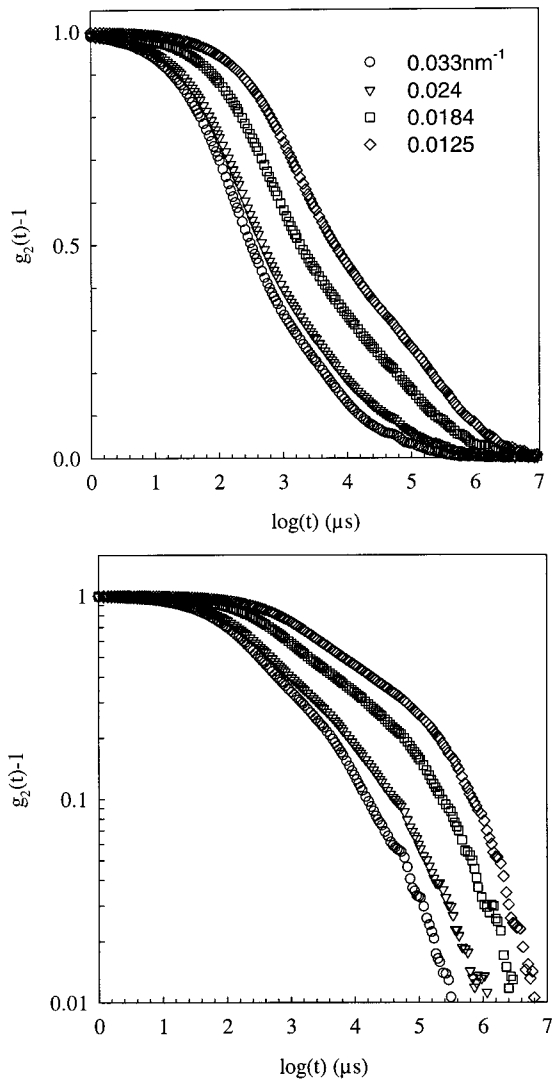

Figure 9. Semilogarithmic (top) and double-logarithmic (bottom) representations of the normalized intensity correlation functions of 15 g/L PIB in ethyl caprylate at different scattering wave vectors indicated in the figure with $T = 288$ K.

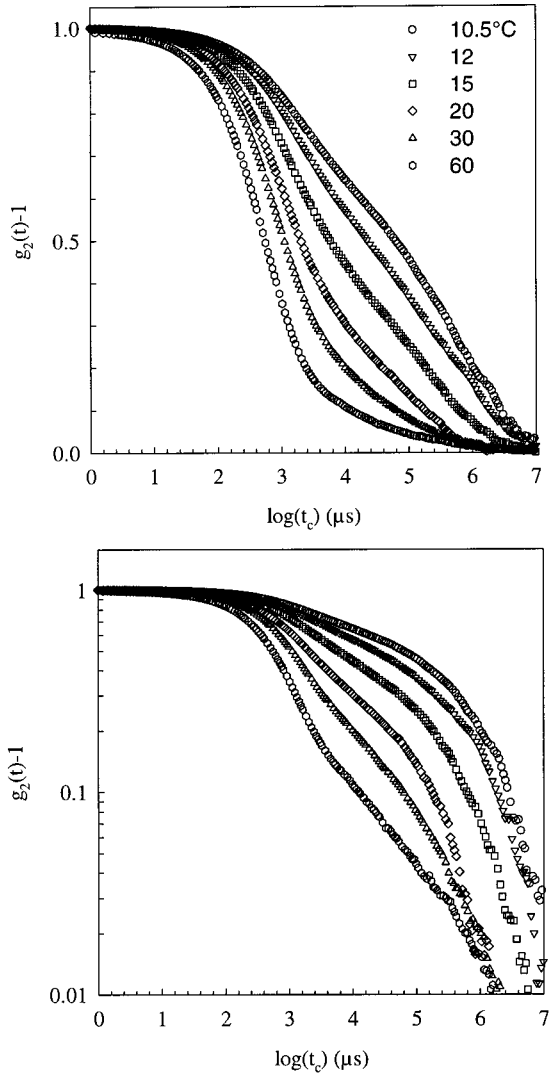

Figure 10. Semilogarithmic (top) and double-logarithmic (bottom) representations of the normalized intensity correlation functions of 15 g/L PIB in ethyl caprylate at different temperatures indicated in the figure with $q = 1.25 \times 10^{-2}$ nm^{-1}. The time is corrected for differences in solvent viscosity and thermal energy: $t_c = t[(\eta(288\text{ K})T)/(\eta(T) \times 288)]$.

Section) and R is the gas constant. For the sample with $C = 15$ g/L M_{os} varies from 160 Pa at $T = 333$ K to 8 Pa at $T = 284.5$ K. If we use for M_{el} the estimated value of 10 Pa, one expects that the relative amplitude of the slow mode increases from about 6% at 333 K to 56% at 283.5 K. These estimates are approximately what we have observed; see Figure 10. Estimates for the other concentrations are also in approximate agreement with DLS results. We cannot make precise comparisons because we do not have precise values of M_{el} or of A_1/A_2.

The effect of the elastic modulus on the correlation function is not restricted to solutions close to T_{ps} but can be detected in good solvents as well albeit with a very small amplitude.[17] In good solvents the static correlation length is smaller than the distance between entanglements, and the dynamics on length scales smaller than ξ are those of single polymer chains. However, close to the phase separation temperature ξ becomes larger than the entanglement distance, and therefore viscoelastic relaxation has an effect on the relaxation of concentration fluctuations already on length scales shorter than ξ. A theoretical treatment of these dynamics has to our knowledge not yet been given.

Conclusion

The experimental results show without ambiguity that entanglements have no effect on the amplitude of critical concentration fluctuations but dominate the dynamics close to T_{ps}. DLS shows a broad distribution of slow relaxation times in addition to a contribution from the cooperative diffusion coefficient. The slow relaxation process is directly related to the viscoelastic relaxation determined by mechanical shear measurements. The values of the terminal relaxation time and the relative amplitude of the slow mode are consistent with existing theory. We observe a q dependence of the slow relaxation which is probably due to the fact that $qR_{gz} > 1$ in the q range covered in the experiment.

The dynamic correlation length (ξ_d) calculated from the cooperative diffusion coefficient is not proportional to the static correlation length. Close to T_{ps} the temperature dependence of ξ_d is dominated by the elastic modulus unless one measures at very low q so that $\tau_1 > \tau_2$. However, the relative amplitude of the fast mode becomes small close to T_{ps} so that it is difficult to determine ξ_d experimentally.

References and Notes

(1) See e.g.: Chu, B. In *Dynamic Light Scattering: Applications of Photon Correlation Spectroscopy*; Pecora, R., Ed.; Plenum Press: NewYork, 1985; Chapter 7.
(2) See e.g.: Sanchez, I. C. *J. Chem. Phys.* **1989**, *93*, 6983.
(3) Ferry J. D. *Viscoelastic Properties of Polymers*, 2nd ed.; Wiley: New York, 1970.
(4) See e.g.: Brown, W.; Nicolai, T. In *Dynamic Light Scattering: The method and some applications*; Brown, W., Ed.; Clarendon Press: Oxford, U.K., 1993; Chapter 6.
(5) Brochard, F.; de Gennes, P. G. *Macromolecules* **1979**, *10*, 1157. Doi, M.; Onuki, A. *J. Phys. II* **1992**, *2*, 1631. Genz, U. *Macromolecules* **1994**, *27*, 5691. Semenov, A. N. *Physica A* **1990**, *166*, 263.
(6) Tanaka, H. *J. Chem. Phys.* **1994**, *100*, 5323.
(7) Nicolai, T.; Brown, W.; Hvidt, S.; Heller, K. *Macromolecules* **1990**, *23*, 5088. Chen, S.-J.; Berry, G. C. *Polymer* **1990**, *31*, 793. Adam, M.; Delsanti, M. *Macromolecules* **1985**, *18*, 1760.
(8) Newman, S.; Krigbaum, W. R.; Laugier, C.; Flory, P. J. *Polym. Sci.* **1954**, *14*, 451.
(9) Huglin, M. B., Ed. *Light Scattering from Polymer Solutions*; Academic Press: London, 1972.
(10) Berne, B.; Pecora, R. *Dynamic Light Scattering*; Wiley: New York, 1976.
(11) Finnigan, J. A.; Jacobs, D. J. *Chem. Phys. Lett.* **1970**, *6*, 141. Moreels, E.; De Ceunick, W. *J. Chem. Phys.* **1987**, *86*, 618.
(12) Szydlowski, J.; Van Hook, W. A. *Macromolecules* **1998**, *31*, 3255.
(13) Melnichenko, Y. B.; Anisimov, M. A.; Povodyrev, A. A.; Wignall, G. D.; Sengers, J. V.; Van Hook, W. A. *Phys. Rev. Lett.* **1997**, *79*, 5266.
(14) Sun, Z.; Wang, C. H. *Macromolecules* **1994**, *27*, 4840. Brown, W.; Stepanek, P. *Macromolecules* **1994**, *27*, 4842.
(15) Wang, C. H. In *Dynamic Light Scattering: The method and some applications*; Brown, W., Ed.; Clarendon Press: Oxford, U.K., 1993; Chapter 5.
(16) Geissler, E. In *Dynamic Light Scattering: The method and some applications*; Brown, W., Ed.; Clarendon Press: Oxford, U.K., 1993; Chapter 11.
(17) Stepanek, P.; Brown, W. *Macromolecules* **1998**, *31*, 1889.

MA9818329